A comparative study of precoding techniques for PAPR reduction of OFDM signals

Abbas Ali Sharifi[1] and Ghanbar Azarnia[2]
[1]*Department of Electrical Engineering, University of Bonab, Bonab, Iran*
[2]*Engineering Faculty of Khoy, Urmia University of Technology, Urmia, Iran*
sharifi@ubonab.ac.ir, g.azarnia@uut.ac.ir
Corresponding author: ***sharifi@ubonab.ac.ir***

Abstract- **Orthogonal frequency division multiplexing (OFDM) is an attractive approach for multi-channel transmission. Due to some advantages such as high spectral efficiency, simplicity in channel equalization, and robustness to the fading channel, the OFDM technique has been generally used in many wireless communication devices. Besides these advantages, the OFDM systems usually experience a high peak-to-average power ratio (PAPR). As a result of the high PAPR, the OFDM signal is clipped during the passing via a non-linear power amplifier. The precoding techniques decrease the autocorrelation of the input data symbols to mitigate the high PAPR. In this paper, we compare WHMT, VLMT, DCMT, DHMT, DFMT, ZCMT, and CVMT precoding approaches in terms of autocorrelation and PAPR reduction performance. We demonstrate that the serial combinations of both ZCMT and CVMT precoding matrices with the IFFT matrix cancel the impact of each other when their dimensions are the same. In this case, a sparse matrix is produced and hence the PAPR of the OFDM signal is remarkably reduced. This issue is proved by the mathematical calculations and verified by the simulation results. It is also presented that DFMT, ZCMT, and CVMT precoding schemes have almost the same PAPR reduction performance and they are the best among their counterparts.**

Index Terms- OFDM, PAPR, Precoding, ZCMT, CVMT

I. INTRODUCTION

The increasing requirements for high data rate wireless equipment make the use of orthogonal frequency division multiplexing (OFDM) to be inevitable [1]. The OFDM technology has some superiorities such as high spectral efficiency, simplicity in channel equalization, and robustness to the fading channel. These superiorities make the OFDM technique to be generally used in many wireless broadband communication devices such as asymmetric digital subscriber line (ADSL),

Manuscript received 12-Jan.-2021 and revised 6-March-2021,
Accepted on 8- April-2021
P- ISSN: 2322-4088
E- ISSN: 2322-3936

digital audio broadcasting (DAB), terrestrial digital video broadcasting (DVB-T), wireless LAN (WLAN) and WiMAX [2]. Besides these advantages, the OFDM signal often experiences a large amplitude variations in the time domain. Since a large number of orthogonal subcarriers are combined with an IFFT procedure. Therefore, an OFDM signal has a high peak-to-average power ratio (PAPR), compared with a single carrier signal. As a result, the OFDM signal, during the passing through a non-linear high power amplifier (HPA), is clipped and hence the overall efficiency is deteriorated and in-band distortion and out-of-band radiation occur. To mitigate such effects, the OFDM transmitter needs an expensive linear HPA with a high dynamic range [3].

The PAPR problem is the most challenging issue of an OFDM system. Several solutions have been reported so far to overcome the PAPR of OFDM systems. Some of these proposals are clipping and filtering [4], non-linear companding [5], block coding [6], tone reservation (TR) and tone injection (TI) [7], precoding [8], [9], [10], partial transmit sequence (PTS) [11], and selective mapping (SLM) [12]. The comprehensive investigations on the PAPR reduction approaches are also reviewed in [13] and [14].

Clipping technique reduces the PAPR by clipping the OFDM signal to a preferred level [4]. This technique is a non-linear and distortion-based PAPR reduction approach. Companding is also a non-linear method to minimize the PAPR. In this method, a compander is applied to the OFDM signal and a decompanding function is used at the receiver to extract the original signal [5]. In the coding technique, a specific code word is used before modulation to reduce the PAPR [6]. In TR and TI approaches, some extra subcarriers are used for PAPR reduction of the OFDM signal [7]. In precoding based PAPR reduction method, a precoder matrix is applied to the constellation symbols and then the IFFT operation is performed [8], [9], [10]. In the PTS technique, the input data frame is partitioned into several sub-frames and each sub-frame is multiplied by a corresponding phase factor. Then, the IFFT of each new sub-frame is computed [11]. The PTS technique is optimal when it explores all probable combinations of phase factors. However, the system complexity is increased exponentially with increasing the number of divided sub-frames. In the SLM technique, the input data frame is multiplied by several phase factor sequences. Then, IFFT procedure is applied to each obtained frame. Finally, the PAPR for the IFFT data output is calculated and the signal with minimum PAPR is sent [12]. Both of PTS and SLM techniques need the transmission of side information to the receiver for correct detection of information symbols, which deteriorates the bandwidth efficiency.

Among these methods, the precoding is very attractive because of its simplicity for implementation and requiring no sending of side information. A precoding technique decreases the high PAPR without any degradation of the bit error rate (BER) performance and any distortion compared with an original OFDM system. Some of the important techniques of precoding are: Walsh-Hadamard matrix transform (WHMT) [15], Vandermonde-like matrix transform (VLM) [16], discrete cosine matrix transform (DCMT) [17], discrete Hartley matrix transform (DHMT) [18], discrete Fourier matrix transform (DFMT) [19], [20], [21], Zadoff-Chu matrix transform (ZCMT) [22], and complex Vandermonde matrix transform (CVMT) [23].

In this paper, we consider the precoding-based PAPR reduction approach. In the precoding scheme, an appropriate precoder matrix is applied to the constellation symbols before the IFFT operation. The main goal of the precoding technique is minimizing the autocorrelation of the input symbols for reducing the high PAPR. When the input symbols are strongly correlated, the OFDM signals have high PAPR. We compare several precoding matrices for PAPR reduction of OFDM signals. The precoding techniques WHMT, VLMT, DCMT, DHMT, DFMT, ZCMT, and CVMT are compared in terms of PAPR and autocorrelation reductions. It is demonstrated that the serial combinations of both ZCMT and CVMT with the IFFT operation cancel the impact of each other when their dimensions are equal. By the multiplication of these precoding matrices with the IFFT matrix, a sparse matrix is produced. The obtained matrix has only one non-zero element in each row and column and hence the PAPR of the OFDM signal is remarkably reduced. In this case, the OFDM signal, similar to the DFT-spreading based single-carrier frequency division multiple access (SC-FDMA), has the same PAPR as the baseband modulated symbols. This issue is proved by the mathematical calculations and verified by the simulation results. Furthermore, we obtain that DFMT, ZCMT, and CVMT precoding schemes have almost the same PAPR reduction performance and they are the best among their counterparts.

The remainder of the paper is prepared as follows: Section 2 briefly describes the OFDM system model and PAPR. The system model of the precoding based PAPR reduction is provided in section 3. In this section, several precoding matrices and the mathematical expression of the autocorrelation function are discussed. Also, the serial combinations of ZCMT and CVMT with IFFT are thoroughly discussed in the same dimensions. In section 4, the performances of different precoding techniques are evaluated through simulation. Finally, section 5 concludes the paper.

II. THE OFDM SYSTEM MODEL AND PAPR

In an original OFDM system, the input source bits are converted to constellation points to generate the input symbols. The information symbols are divided into frames of length K and an N-points IFFT operation (N-points with ℓ times oversampling) is performed to input data blocks ($N = K\ell$). To mitigate both the inter-symbol and inter-carrier interferences, a cyclic prefix (CP) is attached to each frame. Then, the signal is applied to a digital-to-analog (D/A) converter and finally is amplified by a power amplifier. At the receiver side, the received signal is applied to an analog-to-digital (A/D) converter and changed into a digital signal, the extra CP is deleted, and the FFT operation is applied. Finally, demapping procedure is done to reconstruct the original data. The IFFT operation is applied to a frame of K modulated symbols $\mathbf{X}=[X_0, X_1, \ldots, X_{K-1}]^T$ and a time-domain sequence of OFDM symbols $\mathbf{x}=[x_0, x_1, \ldots, x_{N-1}]^T$ is achieved and expressed as:

$$x_n = \frac{1}{\sqrt{N}} \sum_{k=0}^{K-1} X_k e^{j\frac{2\pi}{N}kn} \qquad 0 \le n \le N-1 \tag{1}$$

The presence of a large number of subcarriers causes the time-domain signal to have high PAPR. The PAPR of an OFDM signal is defined as the ratio of the peak power to the average power such as:

$$PAPR = \frac{max\{|x_n|^2\}}{E\{|x_n|^2\}} \tag{2}$$

where $E\{.\}$ denotes the operator of mathematical expectation.

The PAPR reduction performance is frequently evaluated by the complementary cumulative distribution function (CCDF). This function is the probability that the PAPR is greater than the preset threshold $PAPR_0$. The CCDF of the PAPR for an OFDM frame is written as [1]:

$$CCDF = Pr(PAPR > PAPR_0) = 1-(1-exp(-PAPR_0))^N \tag{3}$$

III. PRECODING-BASED PAPR REDUCTION TECHNIQUE

In the precoding technique, the input symbols are transformed to the new symbols by a suitable precoding matrix and then the IFFT operation is performed. The objective is to minimize the autocorrelation of the input symbols before the IFFT operation. The PAPR of the OFDM signal is very high when the input symbols are highly correlated. The autocorrelation of the sequence $\mathbf{X}$ is written as follows [24]:

$$R_{\mathbf{X}}(m) = \sum_{k=0}^{K-1-m} X_{k+m} X_k^* \qquad m = 0, 1, ..., K-1 \tag{4}$$

The absolute autocorrelation function (ACF), λ, for each frame is defined as

$$\lambda = \sum_{m=0}^{K-1} |R_{\mathbf{X}}(m)| \tag{5}$$

The power of signal is defined as

$$\begin{aligned} |x_n|^2 &= \frac{1}{N} \sum_{m=0}^{K-1} \sum_{k=0}^{K-1} X_k X_m^* e^{j\frac{2\pi}{N}(k-m)n} \\ &= \frac{1}{N} \left\{ \sum_{k=0}^{K-1} X_k X_k^* + 2Re\left[\sum_{k=1}^{K-1} e^{j\frac{2\pi}{N}kn} \sum_{m=0}^{K-k-1} X_{m+k} X_m^* \right] \right\} \\ &= \frac{1}{N} \left\{ R_{\mathbf{X}}(0) + 2Re\left[\sum_{k=1}^{K-1} R_{\mathbf{X}}(k) e^{j\frac{2\pi}{N}kn} \right] \right\} \end{aligned} \tag{6}$$

For any complex Z, we have $Re(Z) \le |Z|$ and $\sum_n Z_n \le \sum_n |Z_n|$, thus,

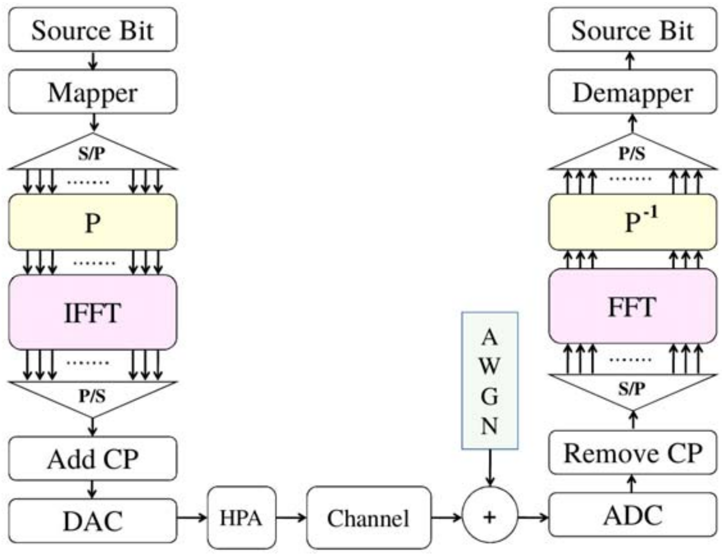

Fig. 1. The system model of precoding-based PAPR reduction of OFDM signals.

$$max\left\{|x_n|^2\right\} \leq \frac{1}{N}\left\{R_{\mathbf{X}}(0)+2\sum_{k=1}^{K-1}|R_{\mathbf{X}}(k)\right\} \tag{7}$$

It is concluded that the peak power of the time-domain OFDM signal $\mathbf{x}$ is proportional to the autocorrelation of the frequency-domain symbols $\mathbf{X}$. Therefore, the input symbols with a lower λ (ACF) have a lower PAPR.

In the precoding approach, each frame of input symbols $\mathbf{X} \in \mathbb{C}^K$, which $\mathbb{C}^K$ denotes the K-dimensional complex vector, is precoded by a precoding matrix $\mathbf{P} \in \mathbb{C}^{K \times K}$. Without precoding, the precoder is an identity matrix. The precoding approaches require no side information for transmission to the receiver. The system model of the precoding technique is shown in Fig. 1. As presented in the figure, each sequence of the input symbols is precoded using a precoder matrix at the transmitter side and the information data is reconstructed at the receiver end by performing an inverse procedure.

The information symbols of length K is precoded by a precoder matrix $\mathbf{P}$ to produce a new vector $\mathbf{Y} \in \mathbb{C}^K$ such as

$$\begin{bmatrix} Y_0 \\ Y_1 \\ \dots \\ \dots \\ \dots \\ Y_{K-1} \end{bmatrix} = \begin{bmatrix} \\ \mathbf{P} \\ Precoder \\ matrix \\ \\ \end{bmatrix} \times \begin{bmatrix} X_0 \\ X_1 \\ \dots \\ \dots \\ \dots \\ X_{K-1} \end{bmatrix} \tag{8}$$

Without oversampling, the IFFT is directly applied to the precoded data $\mathbf{Y}$ and the time-domain OFDM signal, in the output of the IFFT, is achieved as follows:

$$\begin{bmatrix} x_0 \\ x_1 \\ \dots \\ \dots \\ \dots \\ x_{K-1} \end{bmatrix} = \begin{bmatrix} \mathbf{D} \\ IFFT \\ matrix \\ K \times K \end{bmatrix} \times \begin{bmatrix} Y_0 \\ Y_1 \\ \dots \\ \dots \\ \dots \\ Y_{K-1} \end{bmatrix} = \begin{bmatrix} matrix \\ \mathbf{A} \end{bmatrix} \times \begin{bmatrix} X_0 \\ X_1 \\ \dots \\ \dots \\ \dots \\ X_{K-1} \end{bmatrix} \tag{9}$$

where $\mathbf{A}$ is the product of the IFFT matrix $\mathbf{D}$ and precoder matrix $\mathbf{P}$ ($\mathbf{A} = \mathbf{D} \times \mathbf{P}$). Obviously, each element of IFFT matrix $\mathbf{D}$ in the m' th row and n' th column, d_{mn}, is as follows:

$$d_{mn} = \frac{1}{\sqrt{K}} exp(j \frac{2\pi}{K} mn) \tag{10}$$

The element a_{mn} in the m' th row and n' th column of matrix $\mathbf{A}$ is given by:

$$a_{mn} = \sum_{r=0}^{K-1} d_{mr} \, p_{rn} \tag{11}$$

When ℓ-times oversampling is performed, $(\ell - 1)K$ zeros are added to the center of $\mathbf{Y}$ and N-point IFFT ($N = K\ell$) is performed to achieve N coefficients as follows:

$$\begin{bmatrix} x_0 \\ x_1 \\ \dots \\ \dots \\ \dots \\ x_{N-1} \end{bmatrix} = \begin{bmatrix} \mathbf{D} \\ IFFT \\ matrix \\ N \times N \end{bmatrix} \times \left[Y_0, \dots, Y_{\frac{K}{2}-1}, 0, \dots, 0, Y_{\frac{K}{2}}, \dots, Y_{K-1} \right]^T \tag{12}$$

At the receiver side, K information symbols are reconstructed from N coefficients.

A. *Precoding techniques*

WHMT: The elements of the Hadamard matrices are only +1 and -1. The columns and rows are orthogonal to each others. In the WHMT precoding scheme, the kernel can be written as follows:

$$\mathbf{P}_1 = [1], \ \mathbf{P}_2 = \frac{1}{\sqrt{2}} \begin{bmatrix} 1 & 1 \\ 1 & -1 \end{bmatrix}$$
$$\mathbf{P}_K = \frac{1}{\sqrt{K}} \begin{bmatrix} \mathbf{P}_{K/2} & \mathbf{P}_{K/2} \\ \mathbf{P}_{K/2} & -\mathbf{P}_{K/2} \end{bmatrix} \tag{13}$$

The Hadamard matrix satisfies the relation $\mathbf{P}_K \mathbf{P}_K^T = \mathbf{I}_K$.

VLMT: In the VLMT, each element of the precoding matrix in the m' th row and n' th column, p_{mn}, is specified as [16]:

$$p_{mn} = \sqrt{\frac{2}{K+1}} cos(\frac{\pi}{K-1} mn) \qquad 0 \le m, n \le K-1 \tag{14}$$

DCMT: In the DCMT precoding scheme, we have [17]:

$$p_{mn} = \begin{cases} \dfrac{1}{\sqrt{K}} & \begin{cases} m = 0 \\ 0 \le n \le K-1 \end{cases} \\ \\ \dfrac{1}{\sqrt{K}} \cos(\dfrac{\pi}{K}(n+0.5)m) & \begin{cases} 1 \le m \le K-1 \\ 0 \le n \le K-1 \end{cases} \end{cases} \tag{15}$$

DHMT: In the DHMT-based PAPR reduction, p_{mn} is expressed as follows:

$$p_{mn} = \frac{1}{\sqrt{K}}[cos(\frac{2\pi}{K}mn) + sin(\frac{2\pi}{K}mn)] \tag{16}$$

When the dimentions of the DHMT and IFFT are the same ($\ell = 1$), each element a_{mn} of matrix $\mathbf{A}$ is given by [19]:

$$\begin{aligned} a_{mn} &= \sum_{r=0}^{K-1} d_{mr} p_{rn} = \frac{1}{K}\sum_{r=0}^{K-1} exp(j\frac{2\pi}{K}mr)[cos(\frac{2\pi}{K}rn) + sin(\frac{2\pi}{K}rn)] \\ &= \frac{1}{2K}\sum_{r=0}^{K-1}[(1-j)exp(j\frac{2\pi}{K}(m+n)r)] + \frac{1}{2K}\sum_{r=0}^{K-1}[(1+j)exp(j\frac{2\pi}{K}(m-n)r)] \end{aligned} \tag{17}$$

for all integer values of n and r:

$$a_{mn} = \begin{cases} 1 & m = n \;\; and \;\; m+n = 0, K \\ \gamma & m = n \;\; and \;\; m+n \ne 0, K \\ \gamma^* & m+n = K \end{cases} \tag{18}$$

where $\gamma = 0.5(1+j)$.

The matrix $\mathbf{A}$ is sparse and has at most only two non-zero element in each row and column. This matrix is displayed as follows [19]:

$$\mathbf{A} = \begin{bmatrix} 1 & 0 & \dots & \dots & 0 & \dots & \dots & 0 & 0 \\ 0 & \gamma & \dots & \dots & 0 & \dots & \dots & \gamma^* & 0 \\ \dots & \dots & \dots & \dots & \dots & \dots & \dots & \dots & \dots \\ \dots & \dots & \dots & \dots & \dots & \dots & \dots & \dots & \dots \\ 0 & 0 & \dots & \dots & 1 & \dots & \dots & 0 & 0 \\ 0 & 0 & \dots & \gamma^* & 0 & \gamma & \dots & 0 & 0 \\ \dots & \dots & \dots & \dots & \dots & \dots & \dots & \dots & \dots \\ \dots & \dots & \dots & \dots & \dots & \dots & \dots & \dots & \dots \\ 0 & \gamma^* & \dots & \dots & 0 & \dots & \dots & 0 & \gamma \end{bmatrix} \tag{19}$$

DFMT: Clearly, In the DFMT precoding approach, the precoder matrix is an FFT matrix as follows [18]:

$$p_{mn} = \frac{1}{\sqrt{K}} exp(-j\frac{2\pi}{K}mn) \tag{20}$$

Obviously, in the DFMT precoding scenario, the matrix $\mathbf{A}$ is identity matrix.

ZCMT: In the ZCMT precoding scheme, the precoder matrix $\mathbf{P}$ is generated using Zadd-off Chu (ZC) sequence. The ZC sequence $Z = [z_0, z_1, \ldots, z_{L-1}]$ is a mathematical sequence with optimal correlation properties. The first root of ZC sequence with an even length L is written as [22]:

$$z_k = e^{j\frac{\pi}{L}k^2} \quad ; \quad k = 0,1,...,L-1 \tag{21}$$

The precoding matrix is a ZC based row-wise matrix as follows:

$$\mathbf{P} = \frac{1}{\sqrt{K}} \begin{bmatrix} z_0 & z_1 & .. & ..... & .. & z_{K-1} \\ z_K & z_{K+1} & .. & ..... & .. & z_{2K-1} \\ .. & .. & .. & ..... & .. & .. \\ .. & .. & .. & ..... & .. & .. \\ z_{L-K} & z_{L-K+1} & .. & ..... & .. & z_{L-1} \end{bmatrix} \tag{22}$$

where $L = K \times K$. Each element, p_{mn}, for ZCMT precoding matrix is achieved by substituting $k = mK + n$ in equation (13) such as

$$p_{mn} = \frac{1}{\sqrt{K}} z_{mK+n} = \frac{1}{\sqrt{K}} e^{j\frac{\pi}{L}(mK+n)^2} \tag{23}$$

When the dimentions of the ZCMT and IFFT are the same ($\ell = 1$), each element a_{mn} of matrix $\mathbf{A}$ is given by:

$$\begin{aligned} a_{mn} &= \sum_{r=0}^{K-1} d_{mr} p_{rn} \\ &= \frac{1}{K} \sum_{r=0}^{K-1} exp(j\frac{2\pi}{K}mr) exp(j\frac{\pi}{L}(rK+n)^2) \\ &= \frac{1}{K} exp(j\frac{\pi}{L}n^2) \sum_{r=0}^{K-1} exp(j\frac{2\pi}{K}(m+n)r) exp(j\pi r^2) \end{aligned} \tag{24}$$

Obviously, $exp(j\pi r^2) = exp(j\pi r)$ and for each integer value of r we have:

$$\sum_{r=0}^{K-1} exp(j\frac{2\pi}{K}(m+n)r) = 0 \quad if \quad m+n \neq \frac{K}{2} \; or \; \frac{3K}{2} \tag{25}$$

thus,

$$a_{mn} = \begin{cases} exp(j\frac{\pi}{L}n^2) & m+n = \frac{K}{2}, \frac{3K}{2} \\ 0 & otherwise \end{cases} \tag{26}$$

The matrix $\mathbf{A}$ is sparse and has only one non-zero element in each row and column.

CVMT: In the CVMT precoding matrix $\mathbf{P}$, the element p_{mn} is represented as [23]:

$$p_{mn} = \frac{1}{\sqrt{K}} exp(-j\frac{\pi}{2K}(K-2m)(K-2n)) \tag{27}$$

A precoder matrix CVMT is written as follows [23]:

$$\mathbf{P}=\frac{1}{\sqrt{K}}\begin{bmatrix} w^{KK} & w^{K(K-2)} & ... & w^{-KK} \\ w^{K(K-2)} & w^{(K-2)(K-2)} & ... & w^{-K(K-2)} \\ .. & .. & ... & .. \\ .. & .. & ... & .. \\ w^{-KK} & w^{-K(K-2)} & ... & w^{KK} \end{bmatrix} \tag{28}$$

where $w=e^{-j\frac{\pi}{2K}}$.

When the dimentions of the CVMT and IFFT are the same ($\ell=1$), each element a_{mn} of matrix $\mathbf{A}$ is given by:

$$\begin{aligned} a_{mn} &= \sum_{r=0}^{K-1} d_{mr}\, p_{rn} \\ &= \frac{1}{K}\sum_{r=0}^{K-1} exp(j\frac{2\pi}{K}mr)exp(-j\frac{\pi}{2K}(K-2r)(K-2n)) \\ &= \frac{1}{K}exp(jn\pi)\sum_{r=0}^{K-1} exp(j\frac{2\pi}{K}mr)exp(j\pi r)exp(-j\frac{2\pi}{K}nr) \\ &= \frac{1}{K}(-1)^n\sum_{r=0}^{K-1}(-1)^r exp(j\frac{2\pi}{K}mr)exp(-j\frac{2\pi}{K}nr) \\ &= \frac{1}{K}(-1)^n\sum_{r=0}^{K-1}(-1)^r exp(j\frac{2\pi}{K}(m-n)r) \end{aligned} \tag{29}$$

for all integer values of n and r:

$$a_{mn}=\begin{cases} (-1)^n & |m-n|=\dfrac{K}{2} \\ 0 & otherwise \end{cases} \tag{30}$$

The matrix $\mathbf{A}$ is sparse and has only one non-zero element in each row and column. This matrix is displayed as follows:

$$\mathbf{A}=\begin{bmatrix} 0 & ... & ... & 0 & 1 & ... & ... & 0 \\ 0 & ... & ... & 0 & 0 & -1 & ... & 0 \\ ... & ... & ... & ... & ... & ... & ... & ... \\ 0 & ... & ... & 0 & 0 & ... & ... & 1 \\ 1 & ... & ... & 0 & 0 & ... & ... & 0 \\ 0 & -1 & ... & ... & 0 & ... & ... & 0 \\ ... & ... & ... & ... & ... & ... & ... & ... \\ 0 & ... & ... & 1 & 0 & ... & ... & 0 \end{bmatrix} \tag{31}$$

Table 1: Simulation parameters

Parameters	**Values**
Modulation scheme	16-QAM
Number of subcarriers (K)	128
Oversampling factors (ℓ)	1 and 4
N -point IFFT ($N = K\ell$)	128 and 512
Number of frames	10,000

The equations (26) and (30) indicate that when the dimensions of ZCMT/CVMT and IFFT matrices are equal, the multi-carrier transmission vanishes and only single-carrier transmission of information symbols with phase rotation and permutation is achieved. In this case, the ZCMT/CVMT and IFFT operations eliminate the impact of each other and the OFDM signal, similar to the single carrier frequency division multiple access (SC-FDMA) technique in DFT spreading, have the same PAPR as the baseband modulated symbols.

IV. SIMULATION RESULTS

The PAPR reduction performance of the precoding approaches is evaluated using MATLAB software. Numerical simulations are carried out for 10,000 numbers of frames of 16-QAM symbols. The simulation parameters used during this study are listed in Table 1.

Fig. 2 displays the normalized average ACF reduction of the seven precoding matrices. Since the elements of the WHMT are only +1 and -1 and it requires no complex multiplication, it has the worst ACF reduction among the other precoding techniques. In this simulation, the average ACF of 10,000 precoded OFDM frames is calculated and then normalized by dividing to the ACF of the original OFDM. It is seen that the DFMT, ZCMT, and CVMT precoding matrices have almost the same ACF reduction performance and they are the best among their counterparts.

To show that DHMT, ZCMT, and CVMT precoding without oversampling (zero-padding) generate a sparse matrix and eliminate the multicarrier assumption, the PAPR of 16-QAM constellation symbols, original OFDM, WHMT, VLMT, DCMT, DHMT, DFMT, ZCMT, and CVMT for $\ell=1$ are presented in Fig. 3. As discussed before, without zero paddings the dimensions of IFFT and precoding matrix will be equal and the PAPR of 16-QAM modulated symbols and ZCMT/CVMT precoded symbols are identical and the derivations of equations (26) and (30) are verified.

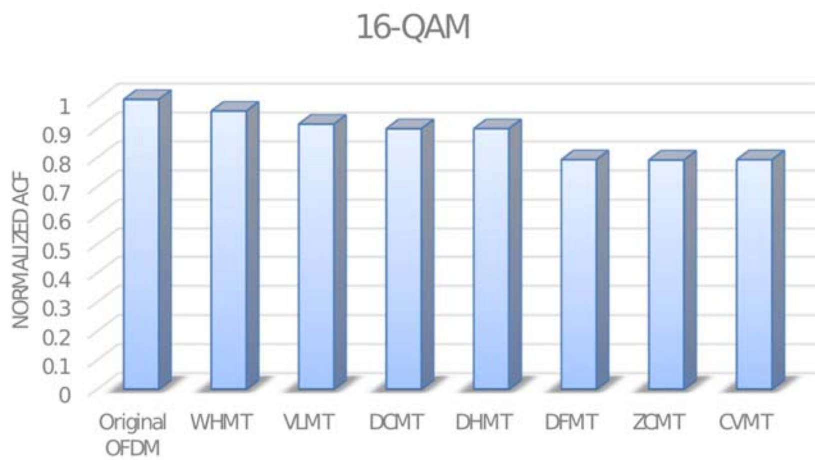

Fig. 2. The average ACF for original OFDM and precoding approaches.

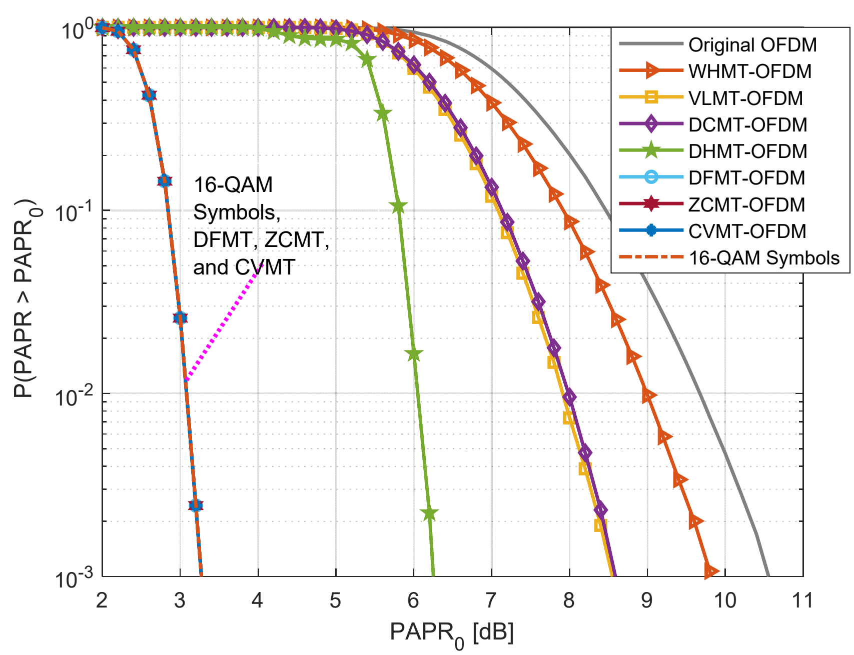

Fig. 3. The PAPR reduction performance of original OFDM and precoding techniques (ℓ =1).

The comparison of the PAPR reduction performance for various precoding schemes is presented in Fig. 4. In this simulation, an oversampling factor of ℓ=4 is used. Similar to the results of Figs. 2 and 3, the PAPR reduction ability of the WHMT scheme is the worst and ZCMT, CVMT, and DFMT precoding techniques have the same and the best PAPR reduction performance.

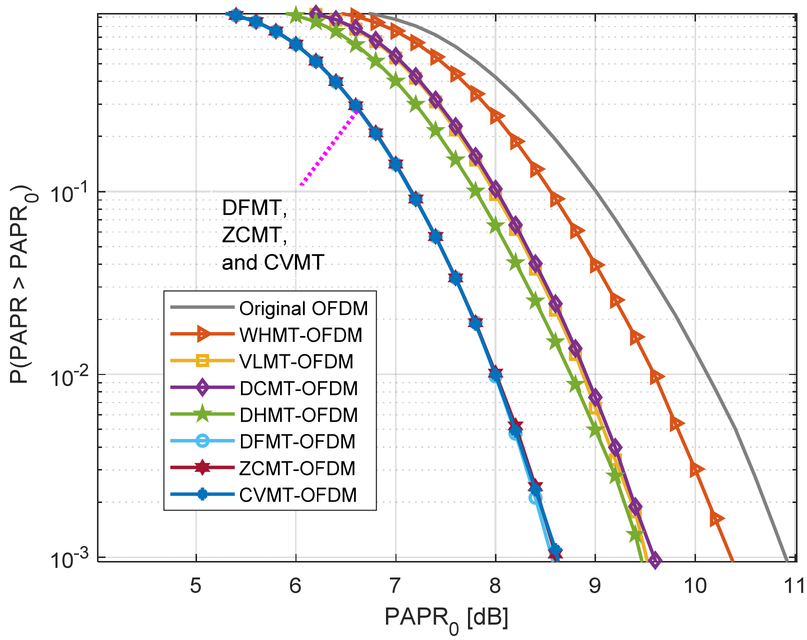

Fig. 4. The PAPR reduction performance of original OFDM and precoding techniques (ℓ =4).

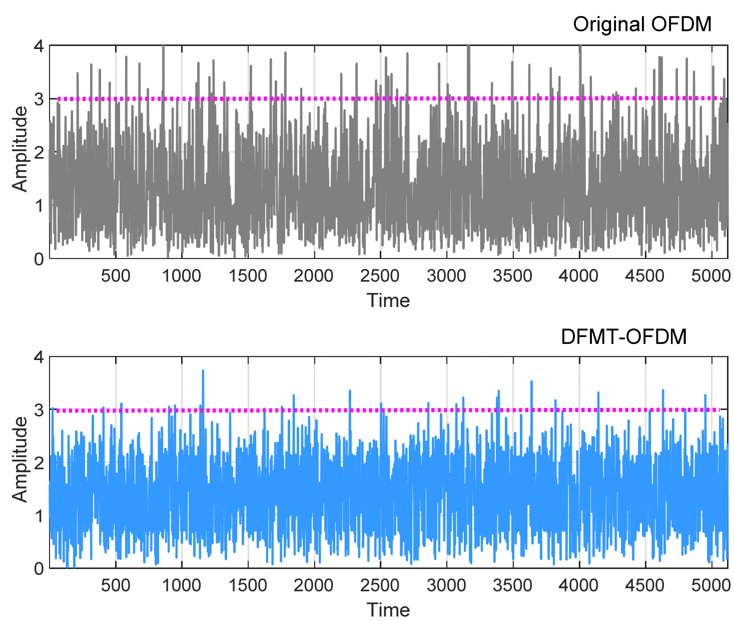

Fig. 5. The time-domain representation of original OFDM and DFMT precoding signals.

Fig. 5 illustrates two time-domain conventional OFDM and precoded signals for 10 numbers of random frames. In this simulation, the precoding is DFMT. As discussed before, the PAPR reduction performance of the DFMT is the same as that of ZCMT and CVMT precodings. Thus, the DFMT approach is selected as a candidate precoding method for this simulation. Each frame of frequency-domain modulated symbols with a length of K =128 is transformed into the time-domain samples of

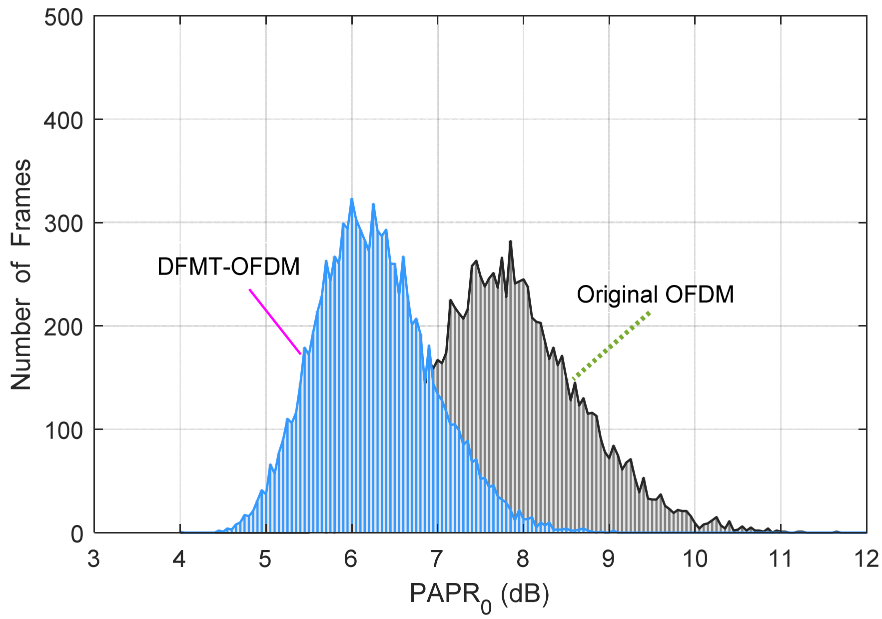

Fig. 6. The histogram of the PAPR for original OFDM and DFMT precoding signals.

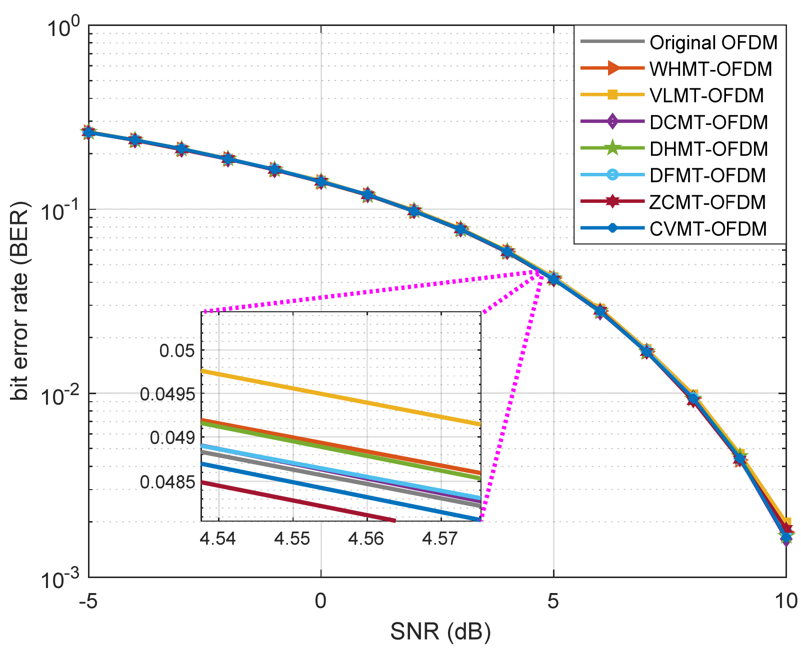

Fig. 7. Bit error rate performance of the original OFDM and precoding techniques.

length 512, after the IFFT operation with an oversampling factor of ℓ=4. This figure shows the amplitude of the original OFDM and DFMT precoded signals. The removal of the undesired large OFDM signal peaks and decreasing the high PAPR are easily recognized.

Fig. 6 illustrates the histograms of random variable PAPR for the original OFDM and DFMT precoded signals for 10,000 numbers of random frames. The obtained results show the high mean for the PAPR of the original OFDM signals and using the DFMT precoding approach, the mean of the variable is significantly reduced. Obviously, the same results can be achieved for both ZCMT and CVMT precoding techniques.

As shown in Fig. 7, by the precoding techniques, the PAPR reductions are achieved without deteriorating the BER performance. In this simulation, an AWGN channel is considered and the SNRs vary from -5dB to 10dB.

V. CONCLUSION

In this paper, the precoding-based PAPR reduction of OFDM signals was thoroughly described. In the precoding approaches, the objective is to decrease the absolute autocorrelation function (ACF) of the input sequence. The PAPR and ACF reduction performances of several precoding techniques such as WHMT, VLMT, DCMT, DHMT, DFMT, ZCMT, and CVMT were compared. We showed that without oversampling in IFFT procedure, the serial combinations of ZCMT/CVMT and IFFT matrices cancel the impact of each other and a sparse matrix is produced. In this case, a single-carrier transmission of information symbols is achieved and the PAPR of the OFDM signal is remarkably reduced. The obtained results also showed that the DFMT, ZCMT, and CVMT have almost the same PAPR and ACF reduction performances and they are the best among others.

REFERENCES

[1] S. Ghazi-Maghrebi, F. Khordadpour-Deylamani, “Evaluation Performance of OFDM Mutlicarrier Modulation over Rayleigh and Rician Standard Channels Using WPT-OFDM Modulations,” *Journal of Communication Engineering,* vol. 6, no. 2, pp. 141-150, July-Dec. 2017.

[2] R. Van Nee, A. De Wild, “Reducing the peak-to-average power ratio of OFDM, in: VTC'98,” *48th IEEE Vehicular Technology Conference. Pathway to Global Wireless Revolution (Cat. No. 98CH36151),* vol. 3, pp. 2072-2076, 1998.

[3] F. Sandoval, G. Poitau, F. Gagnon, “Hybrid peak-to-average power ratio reduction techniques: Review and performance comparison,” *IEEE Access*, vol. 5, pp. 27145-27161, 2017.

[4] K. Anoh, C. Tanriover, B. Adebisi, “On the optimization of iterative clipping and filtering for PAPR reduction in OFDM systems,” *IEEE Access*, vol. 5, pp. 12004-12013, 2017.

[5] S. Peng, Z. Yuan, “A novel criterion for designing of nonlinear companding functions for peak-to-average power ratio reduction in multicarrier transmission systems,” *Wireless Networks*, vol. 24, no. 2, pp. 581-595, Feb. 2018.

[6] T. Jiang, G. Zhu, J. Zheng, “Block coding scheme for reducing PAPR in OFDM systems with large number of subcarriers,” *Journal of Electronics*, vol. 21, no. 6, pp. 482-489, Nov. 2004.

[7] M. Habibi, M. F. Naeiny, “Selective Tone Reservation method for PAPR reduction in SFBC-OFDM systems,” *Journal of Communication Engineering,* vol. 3, no. 2, pp. 109-122, July-Dec. 2014.

[8] S. B. Slimane, “Reducing the peak-to-average power ratio of OFDM signals through precoding,” *IEEE Trans. Vehicular Technology*, vol. 56, no. 2, pp. 686-695, March 2007.

[9] R. Xu, L. Wang, Z. Geng, H. Deng, L. Peng, L. Zhang, "A unitary precoder for optimizing spectrum and PAPR characteristic of OFDMA signal," *IEEE Trans. Broadcasting*, vol. 64, no. 2, pp. 293-306, June 2017.

[10] C.-Y. Hsu, H.-C. Liao, "Generalised precoding method for papr reduction with low complexity in OFDM systems," *IET Communications,* vol. 12, no. 7, pp. 796-808, 2018.

[11] Y. A. Jawhar, L. Audah, M. A. Taher, K. N. Ramli, N. S. M. Shah, M. Musa, M. S. Ahmed, "A review of partial transmit sequence for papr reduction in the OFDM systems," *IEEE Access*, vol. 7, pp. 18021-18041, 2019.

[12] S. Mohammady, R. M. Sidek, P. Varahram, M. Hamidon, N. Sulaiman, "A low complexity selected mapping scheme for peak to average power ratio reduction with digital predistortion in ofdm systems," *International Journal of Communication Systems*, vol. 26, no. 4, pp. 481-494, 2013.

[13] T. Jiang, Y. Wu, "An overview: Peak-to-average power ratio reduction techniques for OFDM signals," *IEEE Trans. broadcasting*, vol. 54, no. 2, pp. 257-268, June 2008.

[14] Y. Rahmatallah, S. Mohan, "Peak-to-average power ratio reduction in OFDM systems: A survey and taxonomy," *IEEE communications surveys & tutorials*, vol. 15, no. 4, pp. 1567-1592, 4th quarter 2013.

[15] M. Park, H. Jun, J. Cho, N. Cho, D. Hong, C. Kang, "PAPR reduction in OFDM transmission using Hadamard transform," *IEEE International Conference on Communications*, vol. 1, pp. 430-433, 2000.

[16] M. M. Hasan, "VLM precoded SLM technique for PAPR reduction in OFDM systems," *Wireless personal communications*, vol. 73, no. 3, pp. 791-801, 2013.

[17] I. Baig, M. Ayaz, V. Jeoti, "On the peak-to-average power ratio reduction in mobile wimax: A discrete cosine transform matrix precoding based random-interleaved orthogonal frequency division multiple access uplink system," *Journal of network and computer applications*, vol. 36, no. 1, pp. 466-475, Jan. 2013.

[18] A. A. Shari, "Discrete Hartley matrix transform precoding-based OFDM system to reduce the high PAPR," *ICT Express*, vol. 5, no. 2, pp. 100-103, June 2019.

[19] A. S. Lakamana, A. M. Prasad, "An effective composite PAPR reduction technique of OFDM by using DFT precoding with piecewise linear companding," *International Conference on Communication and Electronics Systems (ICCES),* pp. 1-6, 2016.

[20] R. Ahmad, A. Srivastava, "PAPR reduction of OFDM signal through DFT precoding and GMSK pulse shaping in indoor VLC," *IEEE Access*, vol. 8, pp. 122092-122103, 2020.

[21] L. Cho, H.-C. Liao, C.-Y. Hsu, "Adjustable PAPR reduction for DFT-S-OFDM via improved general precoding scheme," *Electronics Letters*, vol. 54, no. 14, pp. 903-905, May 2018.

[22] I. Baig, V. Jeoti, "A ZCMT precoding based multicarrier OFDM system to minimize the high PAPR," *Wireless personal communications,* vol. 68, no. 3, pp. 1135-1145, Feb. 2013.

[23] M. M. Hasan, "A novel CVM precoding scheme for PAPR reduction in OFDM transmissions," *Wireless networks*, vol. 20, no. 6, pp. 1573-1581, Aug. 2014.

[24] C. Tellambura, "Upper bound on peak factor of N-multiple carriers," *Electronics Letters*, vol. 33, no. 19, pp. 1608-1609, Sept. 1997.